CHALMERS

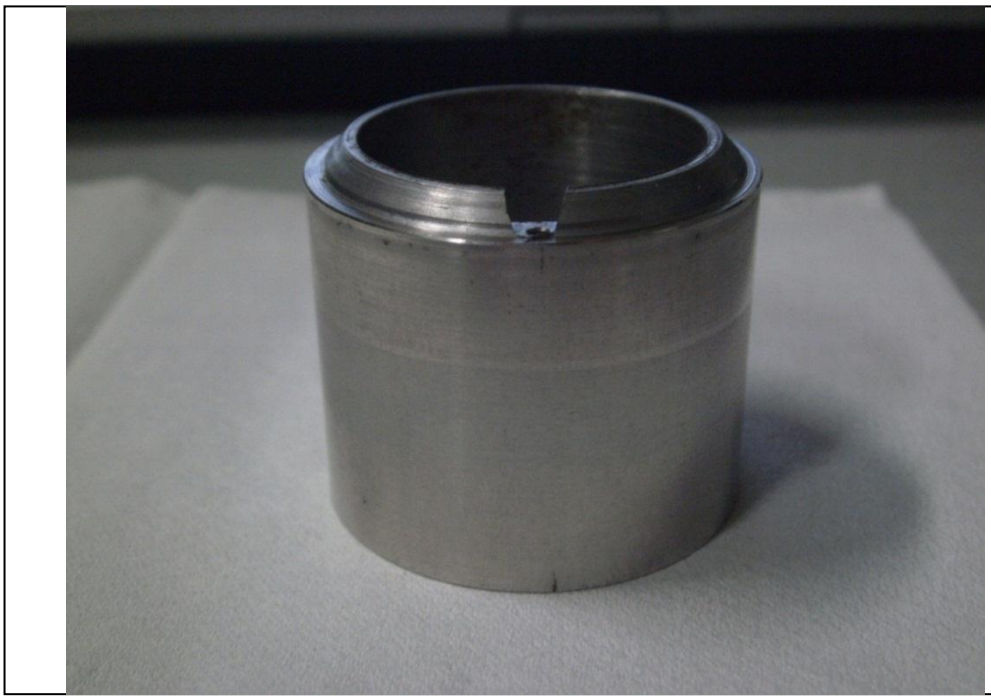

An in plant study of High Temperature Corrosion during Co-combustion of Biomass and Coal.

Master of Science Thesis in the Master Degree Program, Materials and Nano Technology

Sebastian E. Sundqvist

Department of Chemical and Biological Engineering
Division of Energy and Materials
CHALMERS UNIVERSITY OF TECHNOLOGY
Gothenburg, Sweden, 2012

Abstract
In recent years the energy consumption has increased and continues to increase across all types of fuel. The largest part is oil but coal has the second largest consumption. This increase the carbon dioxide concentrations in the atmosphere which leads to that the greenhouse effect is progressing with changing of the climate. Therefore in order to minimize the CO_2 emission to the atmosphere new methods and alternative fuels becomes of major importance. New methods or power plants are a costly investment while an alternative fuel could be comparatively less so. Biomass is one such fuel which is becoming more and more common as fuel in combustion plants for heat and power production.

There are a number of viable sources of biomass and these can be divided into four primary groups

- Woody and woody materials
- Annual growth such as grass, straw and leaves.
- Agriculture byproducts and residues such as rice husks, shells, hulls, pits, and animal manures
- Refuse derived fuels (RDF), waste or non-recyclable papers.

However there are drawbacks with biomass as it contains unwanted components which lead to corrosive deposits formation. The inorganic material in the biomass consists of elements such as Si, K, Na,S, Cl, P, Ca, Mg, Fe. The presence of these elements in the fuel and thus in the boilers can lead to ash fouling and slagging. Furthermore it among other reasons will limit the operation temperature that can be used in order to prevent high corrosion rate. Otherwise the superheater for example will have a shorter lifetime. Shorter lifetime will result in more operation stops in order to change old components, resulting in a large cost for the power production. If more operation stops is necessary then biomass will be considered a unfavorable fuel and less likely to be used in any large scale which would minimize the benefits of using biomass. By using co-combustion the disadvantages of the extremes of either pure coal or biomass are reduced and one benefit is high efficiency.

The aim is to study the initial corrosion on three types of material at high temperature in co-combustion with biomass and coal. This is done with three different fuel mixtures, pure coal and co-combustion with biomass 20% and 40% in a commercial boiler. It's investigated using an air-cooled probe with T22, 304L and Sanicro 28 as the three materials.

Acknowledgement

Professor Jan-erik Svensson, Assistant Professor Jesper Liske and Doctor Dongmei Zhao.
For their guidance, trust and support. For all the time spent and advice given.
For their enthusiasm towards international cooperation.

Associate Professor Yang Hairui
For his guidance, openness, pratical sense and forward spirit.

Associate Professor Katarina Gårdfelt and GMV
For sponsoring my trip and the intrest show for the project.

Ph.D Chao Junnan
For his friendship and openness.
For all the help he has given me in adjusting and in the project.

Student Liu Zhi
For his friendship.
For all he has helped with in the project.

HTC group
For the intrest they have shown in my project.

All other friends and collegues at Chalmers.
For long term intrest in my experince in a foreign country.

My family
For the support and concern.
The intrest in my experience and the welcome home.

Contents

1 Introduction 5
1.1 Background 5
1.1.1 Sources of biomass 5
1.1.2 Co-combustion 6
1.2 Concepts of Corrosion – Theory 7
1.2.1 Oxide formation 8
1.3 Mechanisms of Corrosion 9
1.3.1 Active oxidation 9
1.3.2 Sulpidation 9
1.3.3 Hot corrosion 9
1.4 Previously Done 10
1.5 Aim 10
2 Experiments 10
2.1 Boiler 10
2.2 Procedure 11
2.3 Fuel 13
2.3.1 Coal 13
2.3.2 Biomass 14
3 Analytical techniques 14
3.1 Imaging techniques 15
3.1 Elemental analysis techniques 15
3.1 Phase detection techniques 15
3.2 Analysis Procedure 15
4 Results and discussion 16
4.1 Optical Images 16
4.2 SEM 17
4.3 EDX 20
4.3.1 T22 100% Coal 180° 20
4.3.2 T22 Coal + 40% Biomass 180° 22
4.3.3 Sanicro 28 Coal + 40% Biomass 180° 24
4.3.4 304L Coal + 40% Biomass 180° 26
4.3.5 Cross Sections SEM & EDX 27
4.3.6 Gravimetric results 29
5 Conclusions 31
6 Future work 31
References 32

1 Introduction

1.1 Background

In recent years the energy consumption has increased and continues to increase across all types of fuel. The largest part is oil but coal has the second largest consumption and of that China is responsible for 48% of the coal consumption according to BP Statistical Review of World Energy June 2011[1]. This increase the carbon dioxide concentrations in the atmosphere which leads to that the greenhouse effect is progressing with changing of the climate. Therefore in order to minimize the CO_2 emission to the atmosphere new methods and alternative fuels becomes of major importance. New methods or power plants are a costly investment while an alternative fuel could be comparatively less so. Biomass is one such fuel which is becoming more and more common as fuel in combustion plants for heat and power production. One reason for this is that it quickly regenerates unlike fossil fuels and it's thus considered as a CO_2 neutral fuel. Hence biomass is suitable for environmental sustainable power production and is already used in a number of commercial plants ranging up to more than 100MW.[2] However due to the greater corrosivity of biomass compared to coal, the steam temperatures are lower in biomass fired plants which in turn leads to a decrease in electricity efficiency. As already stated biomass is a renewable fuel and that has a number of benefits like no new sources similar to coal mines have to be found. Though there will be a great need for biomass and the current production of biomass might not be able to satisfy the demand. However it can be cultivated around the plant giving it short transportation distance but there are drawbacks with biomass as it contains unwanted components which lead to corrosive deposits formation.[2] These components such as K and Cl can contribute to an increased rate of corrosion in the plant.[3][4] There have been stated that when biomass is used as fuel there are corrosion problems when exceeding 530-540°C steam temperature.[5][6] This leads to either shorter lifetime of the plant or a need to operate at a lower temperature. Shorter lifetime will result in more operation stops in order to change old components, resulting in a large cost for the power producers.[3] If more operation stops is necessary then biomass will be considered a unfavorable fuel and less likely to be used in any large scale which would minimize the benefits of using biomass. In the other case where lower operating temperature is used the process becomes less efficient when looking at the electricity produced per amount of fuel. Both of these are unwanted and in order to avoid or decrease the effect of such more knowledge is needed. This includes both lab scale studies in order to determine a mechanism for the corrosion process and field experiments to create a model of lifetime. [7]

1.1.1 Sources of biomass

There are a number of viable sources of biomass and these can be divided into four primary groups; [8]

- Woody and woody materials
- Annual growth such as grass, straw and leaves.
- Agriculture byproducts and residues such as rice husks, shells, hulls, pits, and animal manures
- Refuse derived fuels (RDF), waste or non-recyclable papers. [8]

However the last one is often excluded when referring to biomass. The difference between the other three is based on structural composition of hemicellulose, cellulose

and lignin but also on the concentration and composition of inorganic materials.[8] The inorganic material in the biomass consists of elements such as Si, K, Na,S, Cl, P, Ca, Mg, Fe. As mentioned before K and Cl can lead to an increased rate of corrosion which is why those elements and the other elements are undesired in the boiler. [2][3][4][8] The presence of these elements in the fuel and thus in the boilers can lead to ash fouling and slagging.[8] Furthermore it among other reasons will limit the operation temperature as to prevent high corrosion rate.[5] Although its known that KCl is part of the mechanism of selective chlorine corrosion and that there still are unknown aspect of the process. It's also likely that chlorine corrosion isn't the only mechanism involved in the corrosion. This is a hot topic of today and currently under investigation around the world.[9] However some fuels are cleaner than others. According to Hiltunen, Barišić and Coda Zabetta [10] biomass can be divided into three types.

1: Biomass rich in Ca and K but lean in Si
2: Biomass rich in Si but lean in Ca and K
3: Biomass rich in Ca, K and P

[10][11]

Most of the woody fuels are type 1 while type 2 consists of agricultural fuels like rice husks and examples of type 3 are rapeseed cakes and sunflower seeds. Type 1 is considered clean referring to the amount of corrosive agents but woody biomass produce more reactive ashes than coal at the same temperature. Type 2 is more diverse in both combustion properties and chemical composition. Straw and cereals are an example of this as they have high K and Cl content while different from the previous two rice husks produce ashes containing high concentrations of SiO_2. Type 3 fuels produce ashes that melt at lower temperature than the others fuels. This can lead to severe fouling. [10][11]

1.1.2 Co-combustion

There are a number of benefits with co-combustion with biomass and coal compared to pure biomass or pure coal. When using only wood biomass and exceeding 480°C steam temperature rapid corrosion and widespread deposit formation occurs. This leads to high maintenance cost and low efficiency.[12] Pure coal results in high emissions of CO_2 but the sulphur in the coal can lead to sulphidation.[5] By using co-combustion the disadvantages of the extremes are reduced and one benefit is high efficiency. Another is that the low cost of the fuel and short transportation distance of the biomass.[2] Considering that a part of the fuel is biomass and viewed as a CO_2 neutral fuel it's a better way than pure coal combustion.[2][13] There are several ways that co-combustion can be done, direct co-firing, indirect co-firing and parallel combustion. Direct co-firing is done by feeding the biomass into the normal boiler furnace together with coal. The furnace can be fluidized bed, grate or pulverized combustion type.[2] There might be a need for preprocessing of the fuel depending on the type of fuel and the methods could be drying or grinding. The indirect co-firing is when the biomass is gasified and then the resulting gas is fed into the furnace. Parallel combustion works by using biomass for production of steam that then is used with the main fuel to produce power.[2] Biomass may contain undesirable elements as mention before such as K and Cl and one method for pretreatment is leaching. By leaching with water a large fraction of the alkali and chlorine can be removed. As much as 80% of K and Na can be removed using this method but also 90% of the Cl. However only small fractions of S and P can be removed with the method.[14]

1.2 Concepts of Corrosion – Theory

Corrosion is the degradation or breakdown of an engineered material by reaction with its surroundings. One such reaction is oxidation, the metal reacts with the oxygen in the surrounding environment. The reaction is common since most metals are thermodynamically unstable in oxygen rich environment. In the case that a metal is exposed to oxygen in a high temperature environment a reaction occurs in which the metal from an metal oxide. The metal oxide formed depends on which metal it is, the concentration of oxygen and the temperature. The reaction in its simplest form can be expressed as the following formula:

(1) $$Me + O_2 \leftrightarrow MeO_X$$

According to thermodynamics, an oxide will form on the surface of a metal when the partial pressure of oxygen in its surrounding is greater than the equilibrium partial pressure of oxygen for the oxide. This can result in different oxides forming depending on the partial pressure of oxygen in the environment. One case where this is abundantly clear is with the oxidation of iron where the oxide forms layer depending on the partial pressure of oxygen. The most oxygen rich oxide (Fe_2O_3) forms at the environment/oxide interface while at the oxide/metal interface an oxygen poor oxide ($Fe_{1-x}O$) forms. The stability of the formed oxide can be determined from :

(2) $$\Delta G^\circ = -RT \ln\left(a_{Me_xO_y} / a_{Me}\, p(O_2)\right)$$

In the formula $a_{Me_xO_y}$ and a_{Me} are the activities of the oxide and the metal, $p(O_2)$ is the partial pressure of the oxygen gas. From the free energy and the corresponding temperature the Ellingham diagram is constructed. The Ellingham diagrams illustrate the equilibrium dissociation pressures of oxides at different temperatures. The larger negative value of ΔG° the more stable the oxide and the lower the line lie in the diagram. Any metal whose equilibrium line lies lower in the diagram than a certain metal oxide can be used to reduce that oxide. This also gives that from the information in the Ellingham diagram it can be predicted which oxides that will form from an alloy when oxidized at a given pO_2. [7][15]

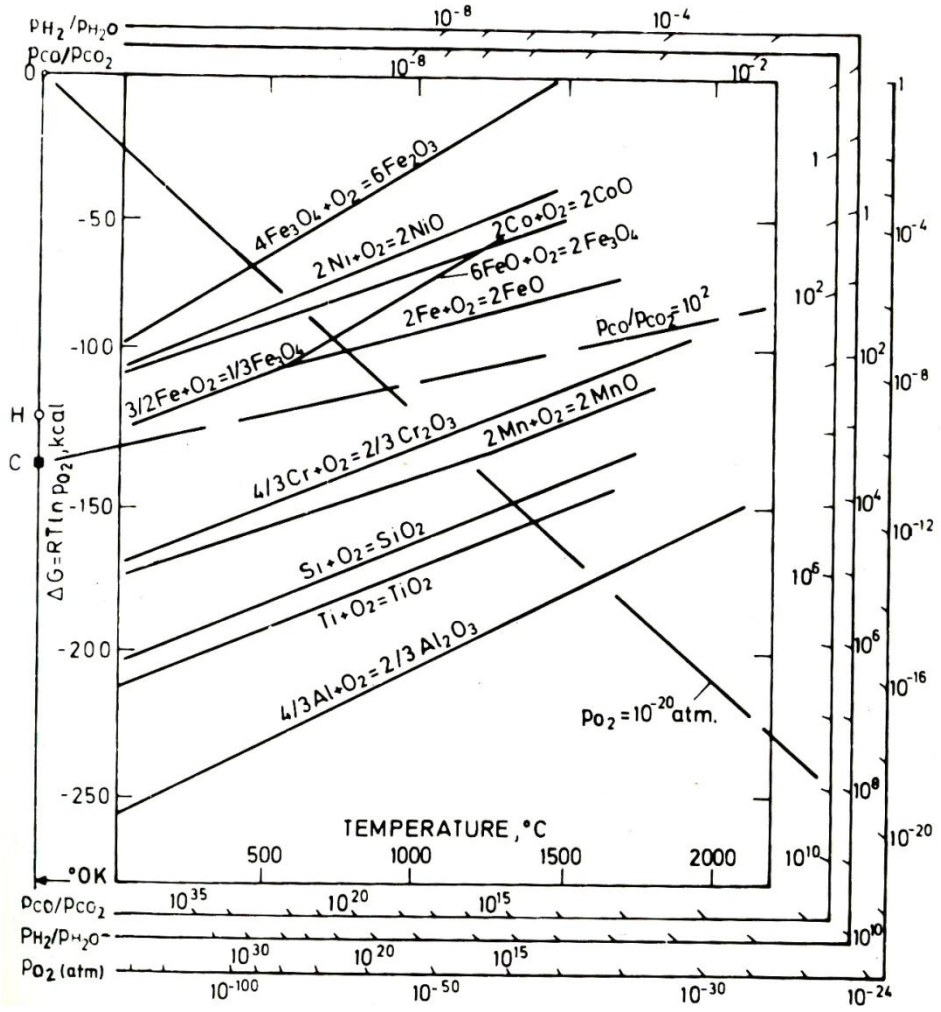

Figure 1 Ellingham diagram.

1.2.1 Oxide formation

When a metal is oxidized and an oxide is formed the initial formation occurs in three steps. First the oxygen molecule adsorbs on the surface and dissociates followed by charge transfer and formation of O^{2-}. Second step is that individual oxide nuclei starts to form and grows laterally until a continuous oxide film has formed. Last is the third step in which the oxide film will continue to grow and increase in thickness. The first two steps are rapid processes where the rate limiting factor is the surface reaction. When the second step is completed and a continuous film has formed the rate limiting factor is changed. At the 3rd stage, the oxide formed separates the metal from the oxygen in the gas phase. Thus the reaction can only proceed through solid phase diffusion of one or both of the reactants. The rate limiting factor is now the diffusion of reactants through the oxide. At ambient temperatures the diffusion is almost zero and the oxide growth would be negligible. When the temperature is increased it leads to a rapid increase in diffusion rate. This causes the oxide to grow and how it grows are depending on the individual reactants diffusion through the oxide. [7][15]

1.3 Mechanisms of Corrosion

There are a number of mechanisms for corrosion, each with their own active elements. Some mechanisms are active oxidation, sulphidation and hot corrosion. Active chlorine corrosion results from the presence of Cl_2 while the other are due to sulphates. [5][16]

1.3.1 Active oxidation

The corrosion can be cause d by a number of Cl containing compounds while HCl and Cl_2 the usual ones. The oxide formed on a metal surface is smooth an act as a protective barrier which slows corrosion since oxygen have to diffuse through the oxide. However when in the presence of Cl_2 the situation changes becuase of the chlorines ability to diffuse through the oxide. It's unclear exactly how it does that but its argued whether it's through pores, crack or grain boundaries. Once the chlorine has penetrated the oxide the reaction occurs in two steps. It can react either according to reaction (3) or (4) depending on whether its Cl_2 or HCl that reacts with the metal to form the metal chlorides. The metal chlorides then evaporate according to reaction (5). The metal could be iron or chromium which would cause problems since that is supposed to form the protective oxide. [16][17]

(3) $$M(s) + Cl_2(g) \rightarrow MCl_2(s)$$

(4) $$M(s) + 2HCl(g) \rightarrow MCl_2(g) + H_2(g)$$

(5) $$MCl_2(s) \rightarrow MCl_2(g)$$

The metal chlorides diffuses to the surface and then can react with oxygen forming solid metal oxides in a loose oxide layer that offers little protection against further attacks. This happens according to reaction (6) and thus a cycle is formed that destroys the protective oxide and progresses the corrosion attack. [16]

(5) $$3MCl_2(g) + 2O_2(g) \rightarrow M_3O_4(s) + 3Cl_2(g)$$

1.3.2 Sulpidation

Sulphidation occurs as a result of alkali sulphates in the deposit but sulphidation can also occure from gaseous environments. In those cases SO_2, SO_3 and S_2 diffuse in the oxide through either micro cracks or vacancies. This results in that sulphidation is much faster than oxidation since it moves through vacancies and there are more vancancies in the sulphide lattice. Sulphidation occures according to reactions (6) and (7). Its stated that in the presence of sulphates there are more sulphidation because of dissociation of $CaSO_4$ which would lead to sulphur reacting with the metal. [5]

(6) $$4M + 3O_2 \rightarrow 2M_2O_3$$

(7) $$2M + S_2 \rightarrow 2MS$$

1.3.3 Hot corrosion

There are many ways to hot corrosion and some of the involve potassium, sulphats and vanadium. Hot corrosion is caused by melts on the surface of the metal but not all of the salts or the responsible compound needs to be molten for hot corrosion to take place. It has been found in [16] that when SO_2 is present with NaCl in Na_2SO_4 then the corrosion rate much higher than if either SO_2 or NaCl were to be absent.[5][16]

1.4 Previously Done

In the field of high temperature corrosion much research has been done both laboratory and in plant studies. Laboratory tests concerns the chemical mechanism which determines the corrosion and what elements leads to corrosion. They have included the effects of compounds such as KCl, K_2SO_4 and real deposits taken from a straw fire boiler. It has also been investigated about the corrosion caused by presence of H_2O with multiple materials.[7][18][19]

In plant experiments or field experiments concerning biomass have involved combustion properties of biomass and corrosion rates depending material temperatures. This has been done for biomass form a number of different sources but also for other possibilities such as animal wastes and municipal wastes. A number of different biomass has been used in several types boilers such as bubbling fluidized bed boilers (BFB), circulating fluidized bed boilers (CFB) and grate fired boilers. [8][10][20]

Other field experiments have focused on the corrosion in co-combustion of biomass and fossil fuels and the composition of deposit on the heat transferring surfaces. It has been investigated which elements that are responsible for the corrosion and what compounds that forms. Another is the possibility of additives such as sulphur and what additional problems or mechanism that occurs. Other addition that have been used is ammonium sulphate introduced in the flue gas to convert KCl to K_2SO_4. [5] [9][12]

1.5 Aim

The aim is to study the initial corrosion on three types of material at high temperature in co-combustion with biomass and coal. This is done with three different fuel mixtures, pure coal and co-combustion with biomass 20% and 40% in a commercial boiler. It's investigated using an air-cooled probe with T22, 304L and Sanicro 28 as the three materials.

2 Experiments

2.1 Boiler

The boiler used in used for the experiment features a single drum, natural circulation, membrane wall and two cyclones. An air pre-heater is used to heat the primary air that is then injected into the wind box, continuing through a two level furnace. The super heater is arranged in a low-temperature section and a high temperature section inside the loopseal.

The boiler has a capacity of 75t/h and the steam pressure is 3.83MPa with a temperature of 450°C. Other temperature such as that of water is 150°C, 20°C for the cold air, 160°C primary air, 175°C secondary air and flue gas temperature is 160°C. The efficiency of the design boiler is more than 81%.

The test location was chosen to after the first set of boiler tubes in the flow path since an earlier placement would be after a turn. That would give a more turbulent flue gas flow and was thereby not chosen.

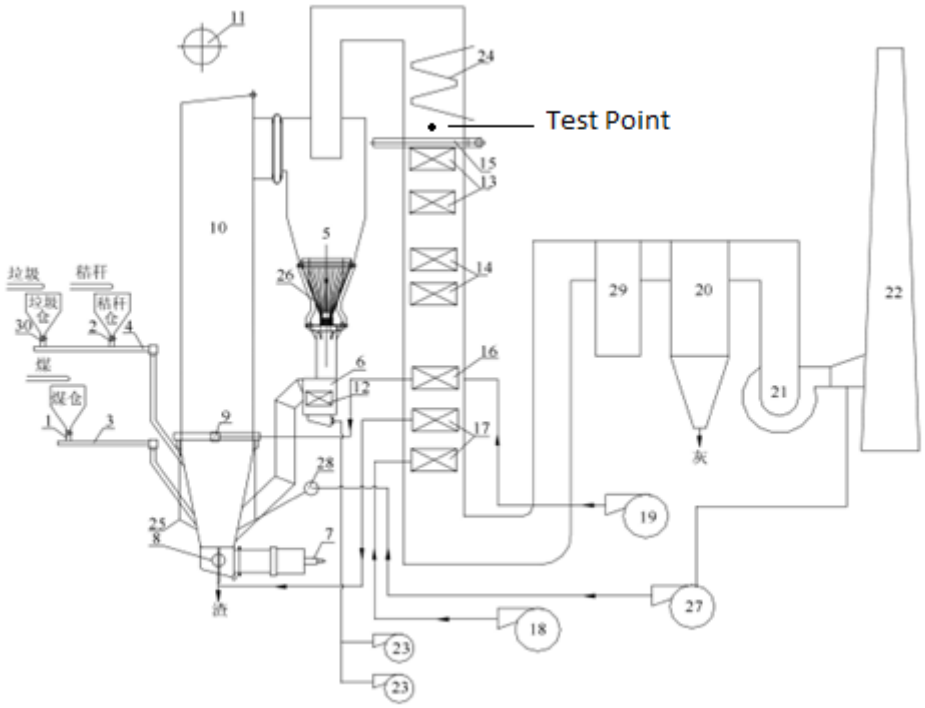

Figure 2 Boiler combustion system 1-coal mouth 2-straw mouth 3-feeder 4-chain plate waste and straw feeder 5-cyclone 6-anti-feeder 7-lgnition 8-primary air 9-secondary air 10-furnace 11-drum 12- super-heater 13-low temperature super-heater 14-economizer group2 15-spray desuperheater 16-secondary air pre-heater 17 primary-air pre-heater 18-primary fan 19 - the secondary fan 20-bag filter 21-air fan 22-Chimney 23-back to feed fan 24-boiler tubes 25- limestone mouth 26 –economizer group 1 27 – recirculation fans 28 -recirculating air inlet 29 –Reactor 30 –waste inlet [21]

2.2 Procedure

The experiment was carried out in a 68 MW commercial fluidized bed boiler in Chengde, China. A 2.1 meter long air cooled probe was used with a diameter of 38 mm. In the front end of the probe six 3 cm long rings were placed. The rings have a outer diameter of 38mm and a wall thickness of 5mm. A 1.2 cm diameter tube with outlets beneath the sample rings runs inside the probe. It delivers compressed air for cooling the sample rings from a gasoline powered air compressor that is separate from the boilers internal compressed air system. The air compressor was connected to a controller box with fast insertion connections and was supplying a constant amount of air to the controller box. Thermocouples were placed in the probe, in the middle ring and outside of the probe, these thermocouples were connected to the controller box. The thermocouple in the middle ring was used to control the temperature of the sample rings and was always installed in such a way that it was facing the flue gas flow. The outer one to measure the flue gas temperature and the inner measure the temperature of the air inside the probe and to confire that the on in the ring was working properly. All temperatures were recorded by a computer installed in the controller box with Eurotherm itools version 7. Around the probe was a spiral tube for the purpose of cooling with water however the water cooling was not used in lack of need and mentioned for accuracy.

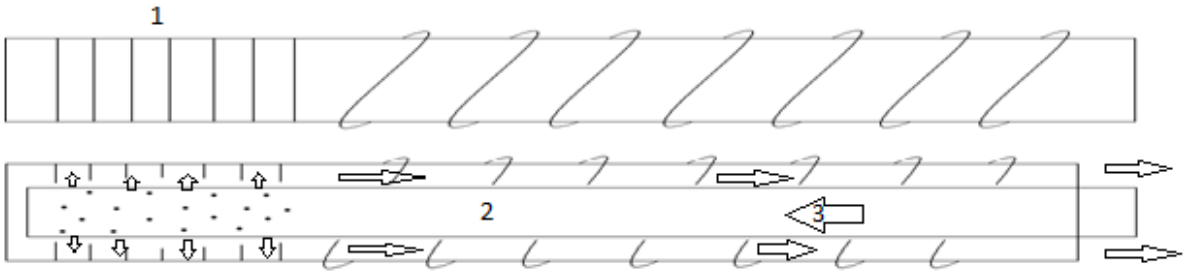

Figure 3 Air cooled probe used with the spiral water cooling tube (water cooling wasn't used). 1) Sample rings placement on the probe. 2) Inner tube in the probe. 3) Air flow direction is indicated by the arrows.

The set temperature for the sample rings were 450°C. Three different cases were investigated based on use of different fuels and three different alloys were selected depending on the Cr content. All rings were weighed and marked with a number and type of alloy before exposure. The alloy 20/gb3087 is a chinese low alloyed steel that have been used in the superheaters in the boiler. As it has low Cr content the low alloyed steel T22 was chosen as a sutible substitute in the experiment. 304L a austenitic stainless steel and Sanicro 28 a high alloyed Fe based steel were chosen because of their higher Cr content and the ratio of Cr/Fe. The alloys and their respective compositons can be viewed in Table 1.

Table 1 Alloys used in the experiment and their respective compositions. Cr/Fe for 20/gb3087 is based on Cr 0.25.

Steel/alloy	Fe	Cr	Ni	Mn	Si	Mo	Cr/Fe
20/gb3087	97	<0.25	< 0.25	0,35-0,65	0.17-0.37	-	0.0026
T22	96	2	-	0.5	-	1	0.02
304L	68	19	10	1.4	0.6	0.5	0.28
Sanicro 28	35	27	31	2	0.7	3.5	0.77

The start of the experiment is considered to be the moment the probe was inserted into the boiler. The flue gas concentration was measured with a portable gas analyzer and also the flue gas velocity. Then the rings were placed on the probe in the order from the front of the probe T22, Sanicro 28 and 304L. The rings were used in doublets. The probe was inserted into the boiler and temperature resistant material was used to seal the gap between the probe and the boiler wall. After observing that the temperature had reached the target temperature the experiment was allowed to continue unsupervised with hourly controls of temperature stability. After 24h the probe was extracted and the target temperature was changed to 40°C so that the controller box would supply maximum amount of air in order for the probe to rapidly cool down. While the probe was cooling the flue gas composition and velocity was measured. When the probe had reached 40°C the rings were removed. Each ring was stored in a separate container with a bottom plate of shockabsorbant material. The containers where then stored in an airtight box with drying agent as to provent any moisture to affect the deposition on the rings. The probe was then fitted with new rings and inserted again. The sample rings were then weighed and one of each doublet was placed in epoxy for transportation and preseravation.

Table 2 Gas composition analysis, measurement of flue gas velocity and particle concentration.

	Before Exposure 1	Between Exposure 1&2	Between Exposure 2&3	After Exposure 3
O2/%	13.1	13.1	13.1	11.8
CO/ppm	0	96	2	12
NO/ppm	136	135	137	140
NO2/ppm	1	1	2	1
NOx/ppm	137	136	138	141
SO2/ppm	0	0	0	42
CO2/%	2.8	4	5.7	15.1
Gas velocity m/s	4.9	4.5	4.5	4.9
particle concentration g/L	0.0026	0.0167	0.0021	0.0146

2.3 Fuel

2.3.1 Coal

The coal used in the boiler is Chifeng and is mined in the area of Chifeng, Inner Mongolia, China. Coal samples were taken from the boiler. Then both combustion and ultimate analysis were performed on the samples. The results from the analysis are displayed in The analysis results are displayed in Table 3.

Table 3 Analysis results for the Chifeng coal, both combustion and ultimate analysis.

Coal	Air dry	Dry	Dry ash free
total moisture %			
moisture %	6.81		
ash %	27.37	29.37	
volatile matter %			
fixed carbon %			
gross calorific value			
net calorific value			
total sulfer %	0.39	0.42	0.59
carbon %	47.39	50.85	72
hydrogen %	3.57	3.83	5.42
nitrogen %	0.62	0.67	0.94
oxygen %	13.85	14.86	21.04
phosphorus %			
chlorine %	0.004	0.004	0.006
Ash		Content	
SiO2 %		61.17	
Al2o3 %		18.98	
Fe2O3 %		6.66	
CaO %		3.56	
MgO %		0.54	
TiO2 %		1.22	
SO3 %		1.32	
P2O5 %		0.52	
K2O %		2.64	

Na2O %	1.54
Amount %	98.15

2.3.2 Biomass

The biomass that was used was wood from Chengde, Hebei, China and samples were taken sent for analysis about elemental composition and ash temperatures. The result are displayed in the following Table 4.

Table 4 Analysis results and ash temperatures of the wood biomass from Chengde.

Wood	
Mar%	15.46
Aar%	2.11
Var%	58.45
FCar%	23.98
Qar,net,p kJ/kg	17452
Car	44.47
Har	5.39
Oar	49.84
Nar	0.33
Sar	0.012%
Clar	0.019%
SiO2	35.58
CaO	21.28
MgO	6.21
Na2O	0.88
K2O	1.51
Al2O3	11.44
TiO2	0.14
Fe2O3	8.74
DT ℃	1100
ST ℃	1200
FT ℃	>1200

3 Analytical techniques

In order to analyze the samples more than one method is required since no single technique obtains sufficient information to determine the process of corrosion. The available methods are imaging techniques, elemental analyzing techniques and phase detection techniques. Imaging techniques as SEM (Scanning Electron Microscopy) can be used to get a rough estimation of the thickness and characteristics of the surface, whether it is deposition or corrosion product. As imaging techniques can´t provide any information about either elemental composition or distribution of respective element other methods are required. A common method for elemental composition is EDX (Energy Dispersive X-rays) but can also be used to do elemental mapping of the sample. Elemental mapping will display each element in an area of the sample and hence the distribution of the respective elements can be obtained. However only knowing the

elemental distribution is not enough to fully explain the corrosion process. In order to describe the corrosion process and growth of the oxide knowledge of the phase is required. Phase detection techniques such as XRD (X-Ray Diffraction) can provide the required information. [7]

3.1 Imaging techniques

There are two types of imaging techniques, optical microscopy and electron microscopy. The principle is the same for both, particles reflect of the sample and is detected which is then used to create and image of the surface of the sample. Optical microscopes use photons as the particle and are generated by an ordinary lamp. There is not sample requirement for use in optical microscopes. In electron microscopes the particle is electrons which can be supplied by an electron gun. Since the electrons strongly interact with matter the electron microscopes has to be operated in vacuum. This leads to sample requirements such as be able to conduct electrons (avoid charging effect) and to be able to endure vacuum. [7]

3.1 Elemental analysis techniques

To have an image of the surface is good but not enough to describe how the reaction has progressed and how it began. In order to obtain the necessary information to determine possible reaction paths elemental analysis is the next step. One such method is EDX as mentioned before and can provide information about the elemental composition, the distribution of these elements and the relative amounts of them. EDX is a nondestructive method which is always used in combination with an electron microscope. The electrons used reaches a depth of >1 μm and the EDX detector makes it possible to split the image into its constituents which will show how the elements are distributed over the surface. However EDX as well as all other elemental analysis techniques are unable to detect which compounds the elements form. For determining which compounds are present phase detection techniques are required. [7]

3.1 Phase detection techniques

XRD is a phase detection technique which illuminates a crystalline compound with x-rays. When the x-rays interact with the sample it produces a unique diffraction pattern depending on the atoms and their placement in the unit cell. No sample preparation is needed and the method doesn't harm the sample. The method investigates a larger area of the sample and gives an overview of the compounds present but cannot be used to investigate localized features. [7]

3.2 Analysis Procedure

The exposed samples were first photographed for documentation. After which SEM-EDX was performed. The only sample preparation that was done was to blow away loose deposit as to prevent it from clogging up filters in the vacuumpump. While this sound rough nothing could be seen to be removed as the instrument used provided a soft wind and there were little loose particles. The sample ring was then placed in the vacuum chamber on a metal plate as to prevent it from moving. The analysis was done on both windside 0° and back 180°. This was done since all the deposit was located on the 180° side while 0° the windside was the primary objectiv. The steps of the analysis was to first do overview pictures of the surface and then magnify and take another

picture. The magnification varies some between the samples depending on the charging effect and whether a clear picture could be taken. Then two EDX spot analysis was done with 10kV acceleration voltage and then two more with 20kV. After that a EDX mapping was done.

4 Results and discussion

4.1 Optical Images

The surface on the windward side (i.e. facing the flue gas at 0°) of the exposed samples show little or no deposit, see fig 4. This is true for all tested material types as well as the three exposure cases. The surface colour of the samples is the same for the different samples, i.e. dull grey. All the samples have lost the metallic shine that the samples had before the experiments. This indicates that there has been a reaction of the surface and an oxide has formed. Due to the lack of metallic shine, the thickness is estimated to be above 0.3µm. No difference of the surface can be seen between high and low Cr containing materials.

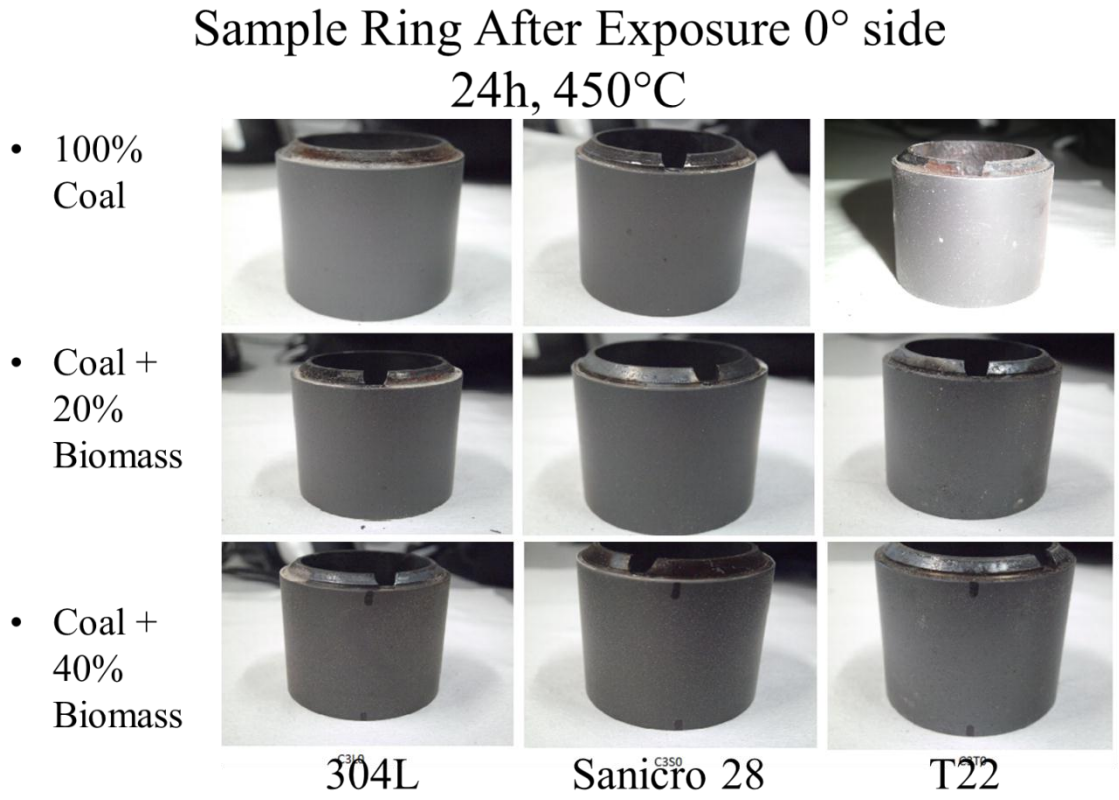

Figure 4 Optical images of the wind side (0°) after 24h at 450°C material temperature for the three materials T22, 304L and Sanicro 28 for the three cases 100% Coal, Coal + 20% Biomass and Coal + 40% Biomass.

On the leeward side, i.e. 180° towards the direction of the flue gas, deposit formation is detected on the sample surface in some cases, see fig 5. All T22 samples show deposit on the surface and the surface has a distinctly different appearance in regards to the other samples. Both 304L and Sanicro 28 have some deposit in the coal + 20% biomass case but not in the 100% coal case or the 40% biomass case. The surface of the samples is different from each other rather than resembling one another as for the wind side.

However, all of the surfaces look different from the samples before exposure where the surface only showed the metallic shine. There were two distinctly different surfaces, one for the low Cr containing material T22 and one for the Cr rich ones 304L and Sanicro 28. In the coal + 20% biomass case as well as the coal + 40% biomass case there is this clear distinction on the surfaces between the materials, Cr rich or poor. However the surface looks different for each material in the 100% coal case. The difference can be explained as mention with the Cr content of the material since it results in a slow growing oxide and the results in the difference in the surfaces. Why there is a difference between the Cr rich materials 304L and Sanicro 28 in the 100% coal case is undetermined.

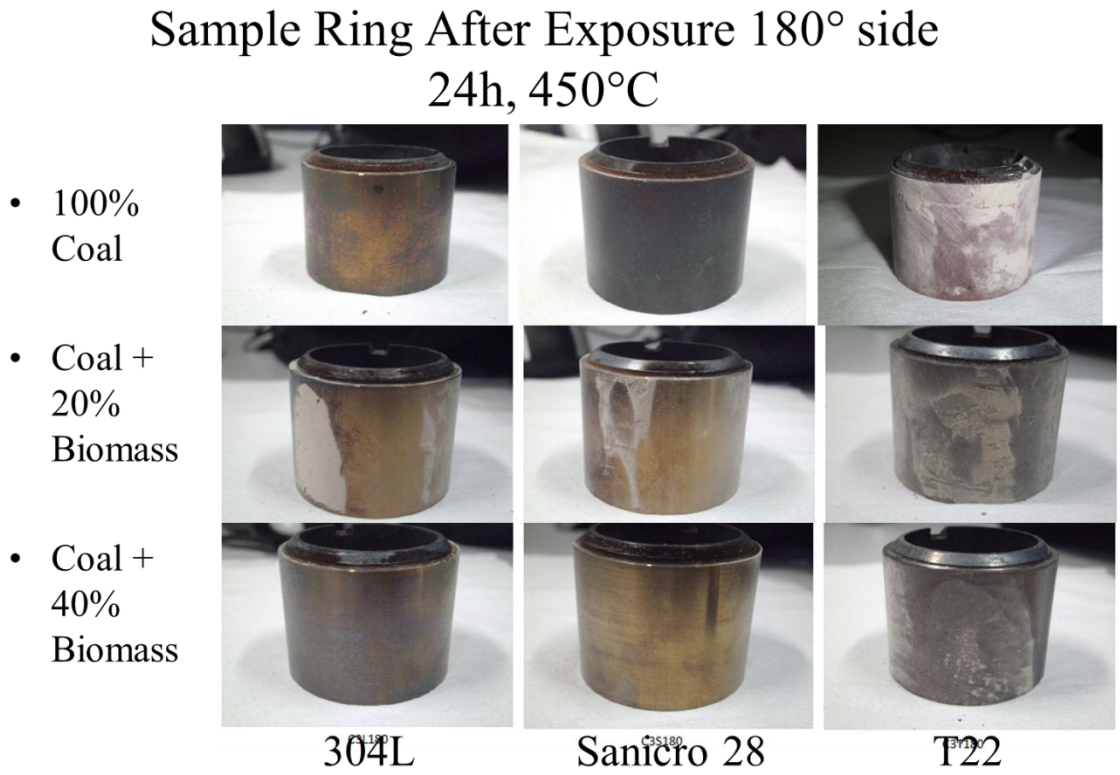

Figure 5 Optical images of the lee side (180°) after 24h at 450°C material temperature for the three materials T22, 304L and Sanicro 28 for the three cases 100% Coal, Coal + 20% Biomass and Coal + 40% Biomass.

4.2 SEM

Figure 6 shows SEM images of the T22 samples with 100% coal and coal with 40% wood biomass. In both cases, the sample surface is smooth on the windward side, lacking a deposit layer. There are however small amount of particles on the windward side surface, seen in the SEM image. The leeward side surface has a lot of deposit for both of the cases. There are some larger particles on the surface. From the SEM analysis, there are no clear differences between T22 exposed in the 100% coal case and the coal + 40% biomass.

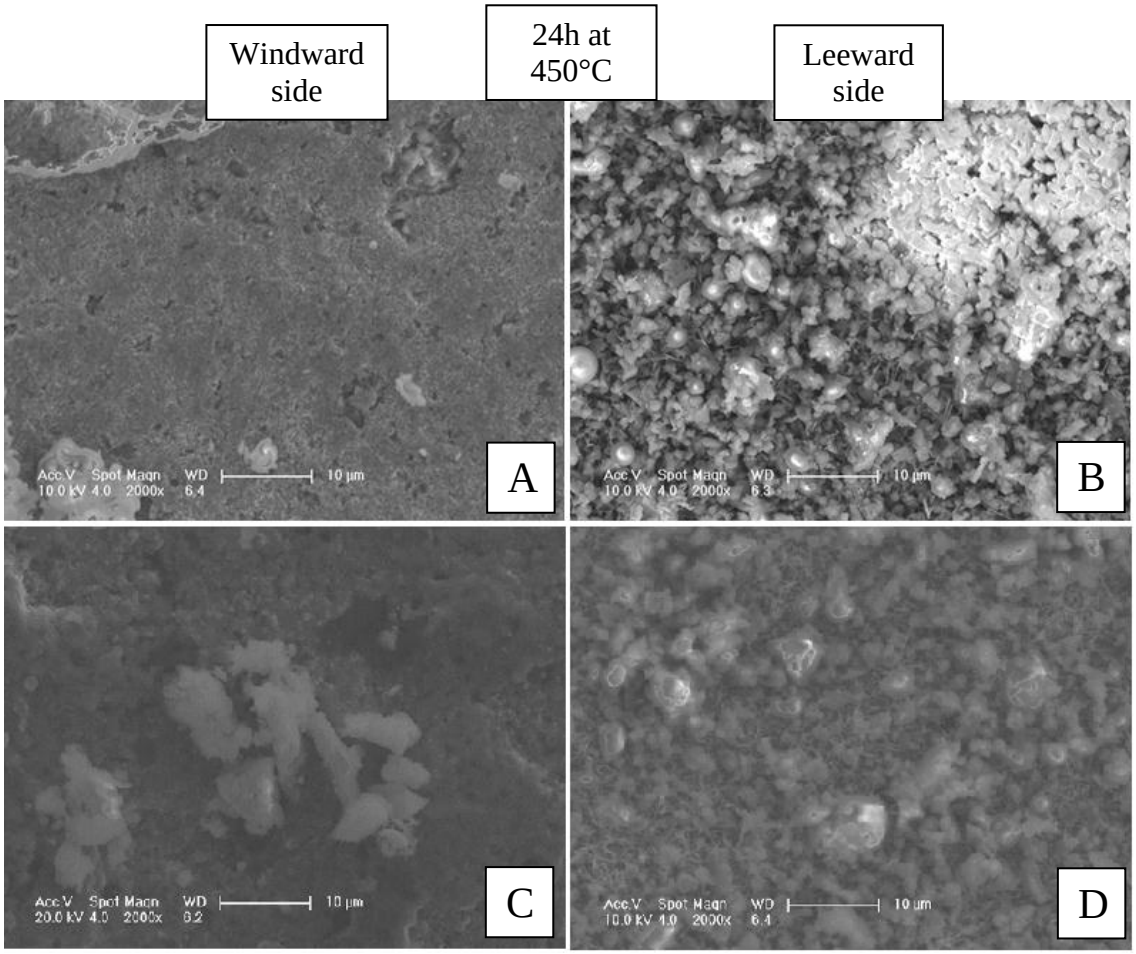

Figure 6 A) T22 100% Coal 0° B) T22 100% Coal 180° C) T22 Coal + 40% Biomass 0° D) T22 Coal + 40% Biomass 180°.

Figure 7 shows SEM images of all three materials T22, Sanicro 28 and 304L for the coal + 40% biomass case. The surfaces on the wind ward side of all the materials are similar. However there are large particles on the T22 sample that is not found on the other two materials. There is also a different surface roughness and topography. The low alloyed material (T22) has a smoother topography than the Cr rich materials. The Sanicro 28 and 304L materials are very similar. The surfaces of these two are very similar in roughness of the surface, the topography seen in the SEM images. On the lee side the Cr rich materials have no deposit only single particles. There is however deposit on the leeward side of the T22 samples. On both 304L and Sanicro 28 surfaces there are small pits and scratches.

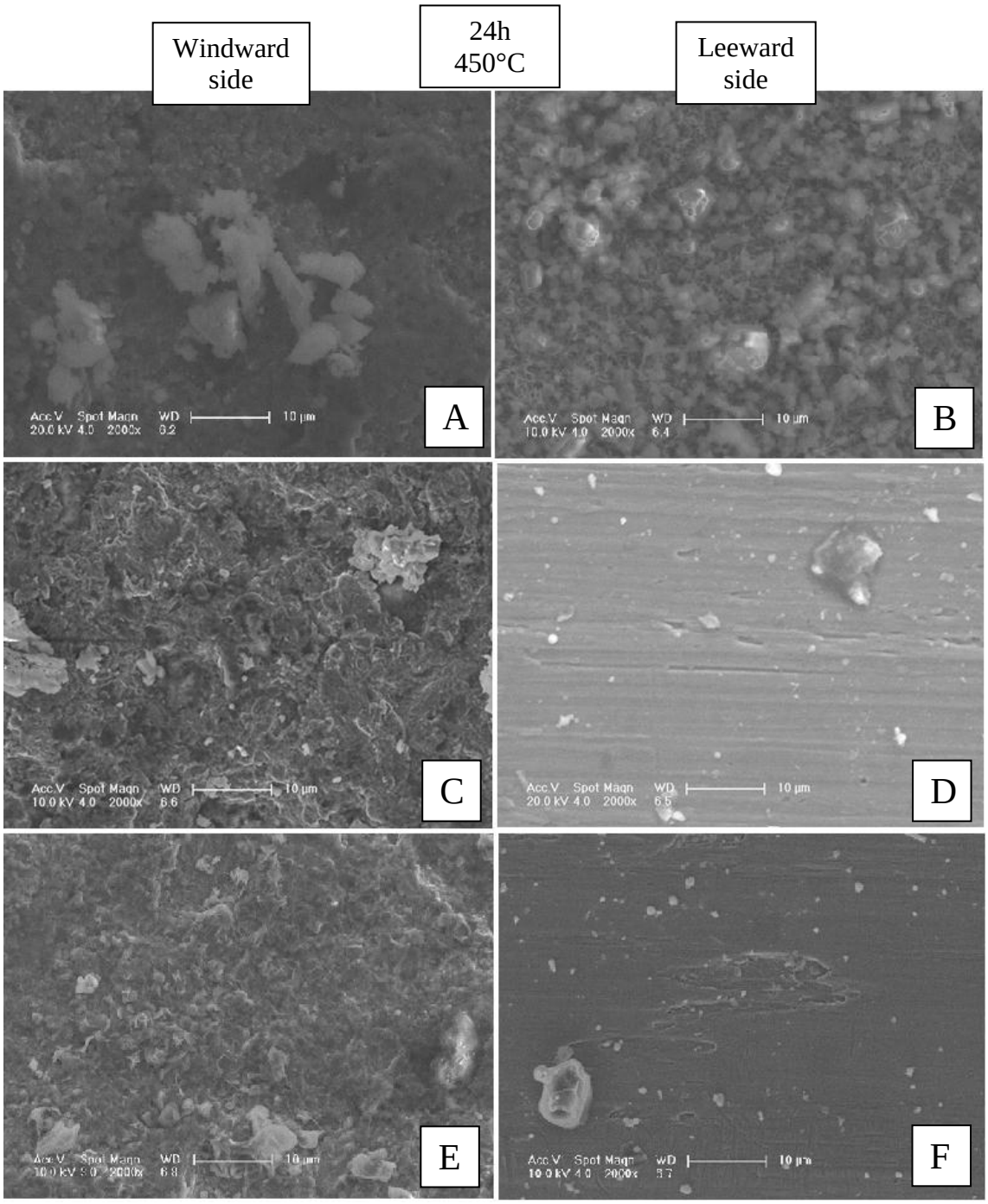

Figure 7 A) T22 Coal + 40% Biomass 0° B) T22 Coal + 40% Biomass 180° C) Sanicro 28 Coal + 40% Biomass 0° D) Sanicro 28 Coal + 40% Biomass 180° E) 304L Coal + 40% Biomass 0° F) 304L Coal + 40% Biomass 180°.

Figure 8 show an SEM image of the T22 sample exposed in the 100% coal case and the spots that were analysed with EDX spot analysis. The quantitative results from the spot analysis are displayed in Table 5. According to the analysis, the surface consists mostly of O, Al and Si. The deposit was homogenous. There are only small differences between the spots. The differences included elements such as C, Al, Ca and Fe. There was no Cl found in any of the spots. There were also minimal amounts of K in the middle position.

4.3 EDX

4.3.1 T22 100% Coal 180°

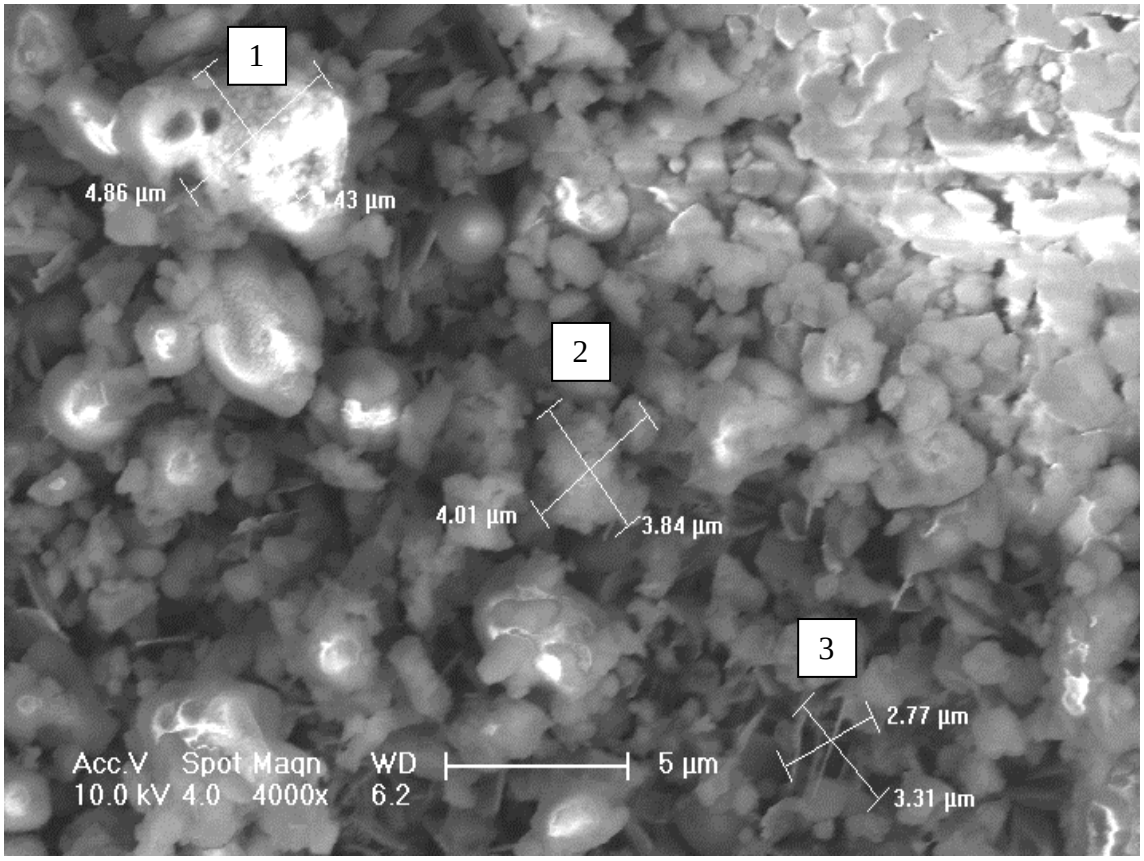

Figure 8 SEM picture of 100% Coal T22 180 side with spots that were analysed.

Table 5 EDAX ZAF Quantification for Case 1 T22 180.

	Element At%											
Positon	C	O	Na	Mg	Al	Si	P	S	K	Ca	Ti	Fe
1	0	61	2	2	11	15	1	0	0	6	1	2
2	0	53	2	1	13	24	0	1	1	2	0	3
3	8	60	2	1	4	15	0	1	0	0	0	9

In Figure 9 and Figure 10, the elemental maps of the lee ward side of T22 100% coal is shown. The images indicate that the surface consists of C, O, S, Si and Al. There is some Ca on the surface. Very little Fe can be detected which is consistent with a covering layer of deposit. There is some S and Ca that coincides in some spots on the surface indicating the presence of $CaSO_4$ in the deposit. Otherwise the deposit is homogenous across the surface. There were no K or Cl found in the deposit with the EDX maps.

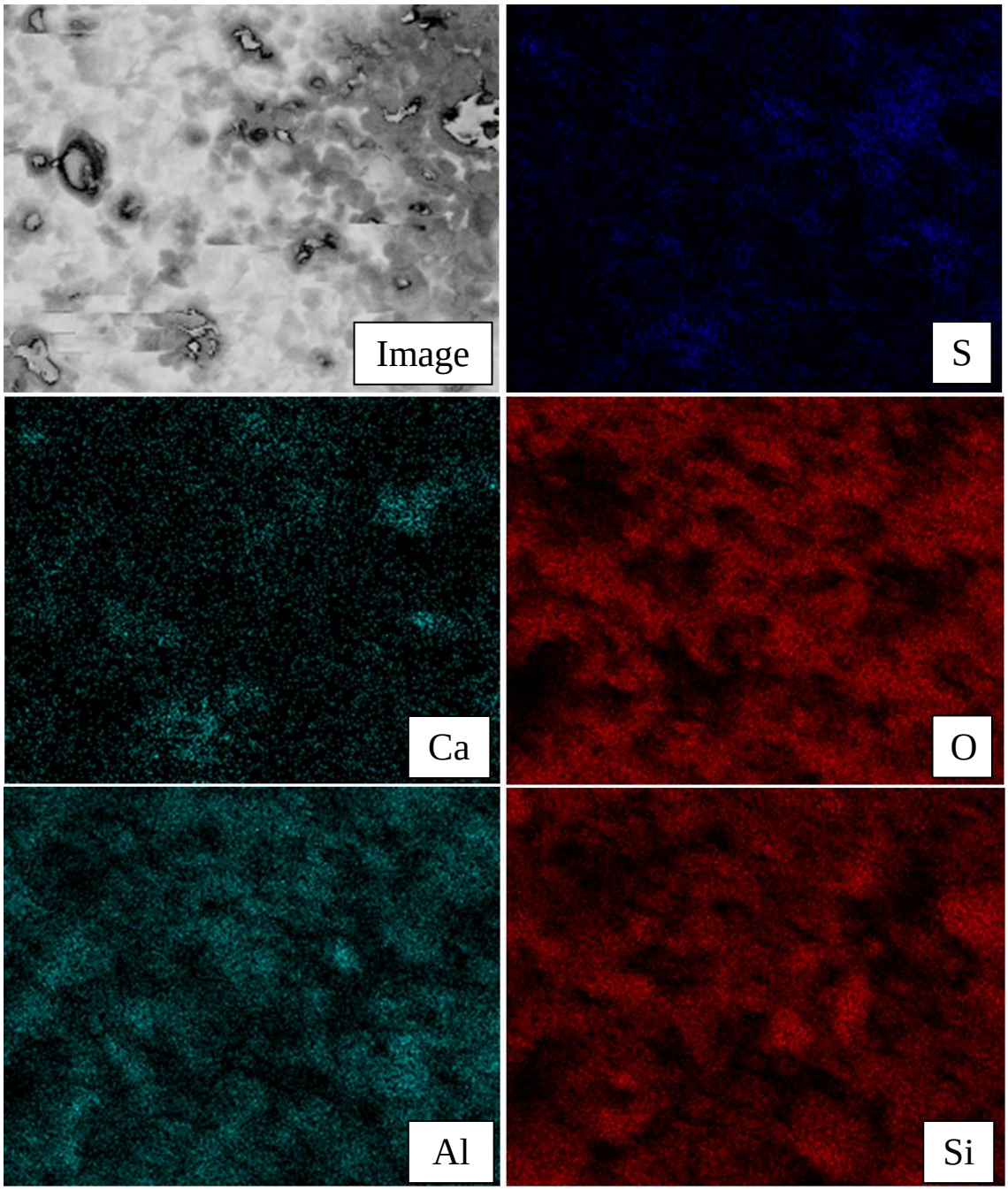

Figure 9 EDX elemental mapping 100% Coal T22 180 side.

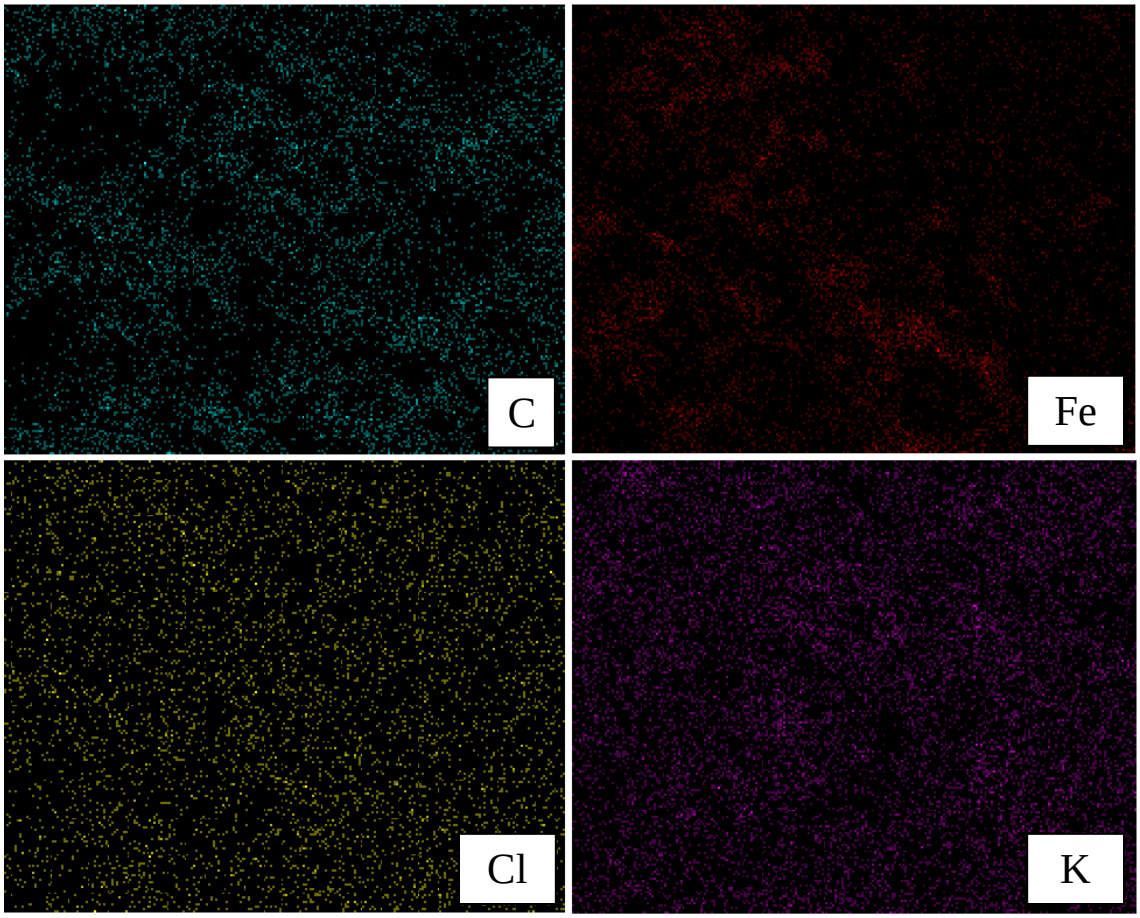

Figure 10 EDX elemental mapping 100% Coal T22 180 side.

4.3.2 T22 Coal + 40% Biomass 180°

Figure 11 and Figure 12 show T22 coal + 40% biomass 180° and the surface consists of Ca, O, S, Al, Si and Fe. There is no K, Cl or Na on the surface in this case either, same as previous case 100% coal with T22. From the EDX Image in Figure 11 and Figure 6**Error! Reference source not found.** previous it can be seen that there are deposit on the surface. The EDX results confirm that the deposit formed on the T22 sample exposed in the in the coal + 40% wood biomass case is homogenous. This shows that the coal + 40% biomass case is the same or similar to the 100% coal case in regards of the deposit composition and homogeneity.

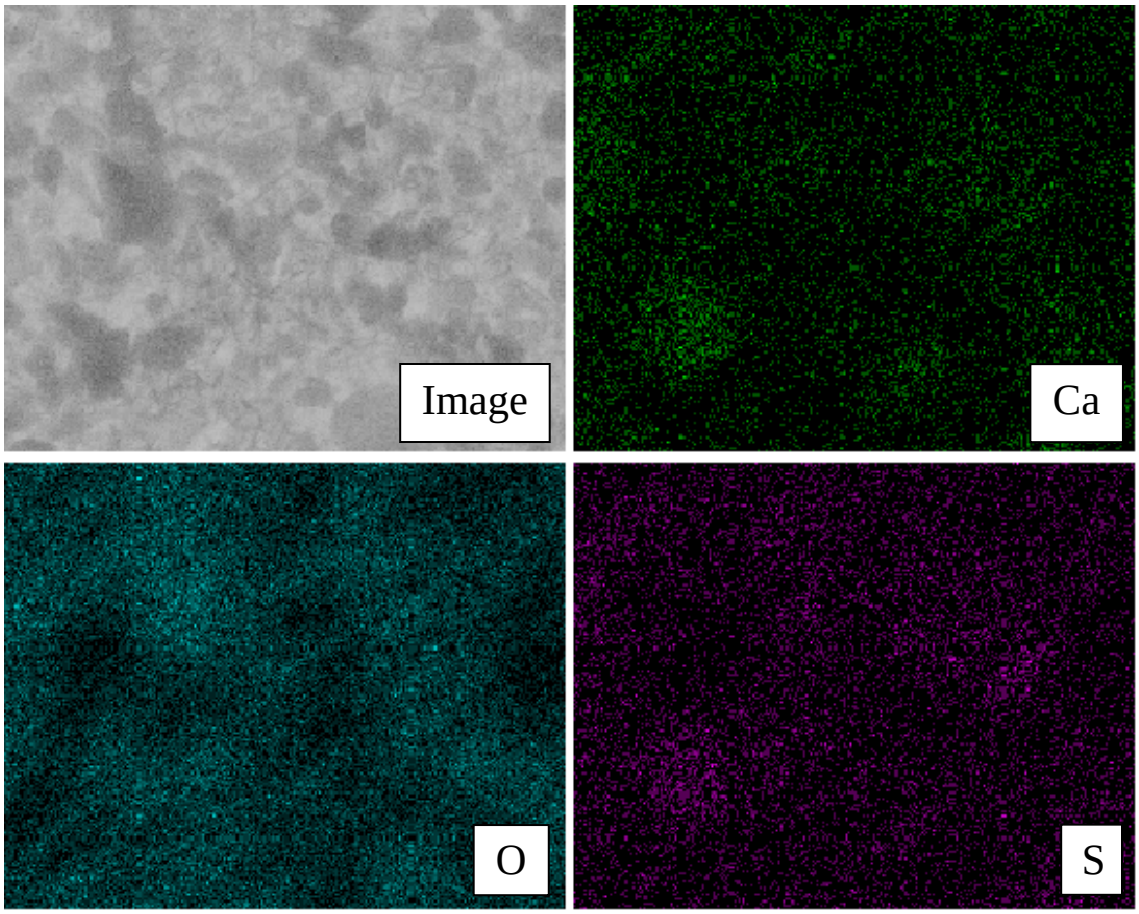

Figure 11 EDX elemental mapping Coal + 40% Biomass T22 180 side.

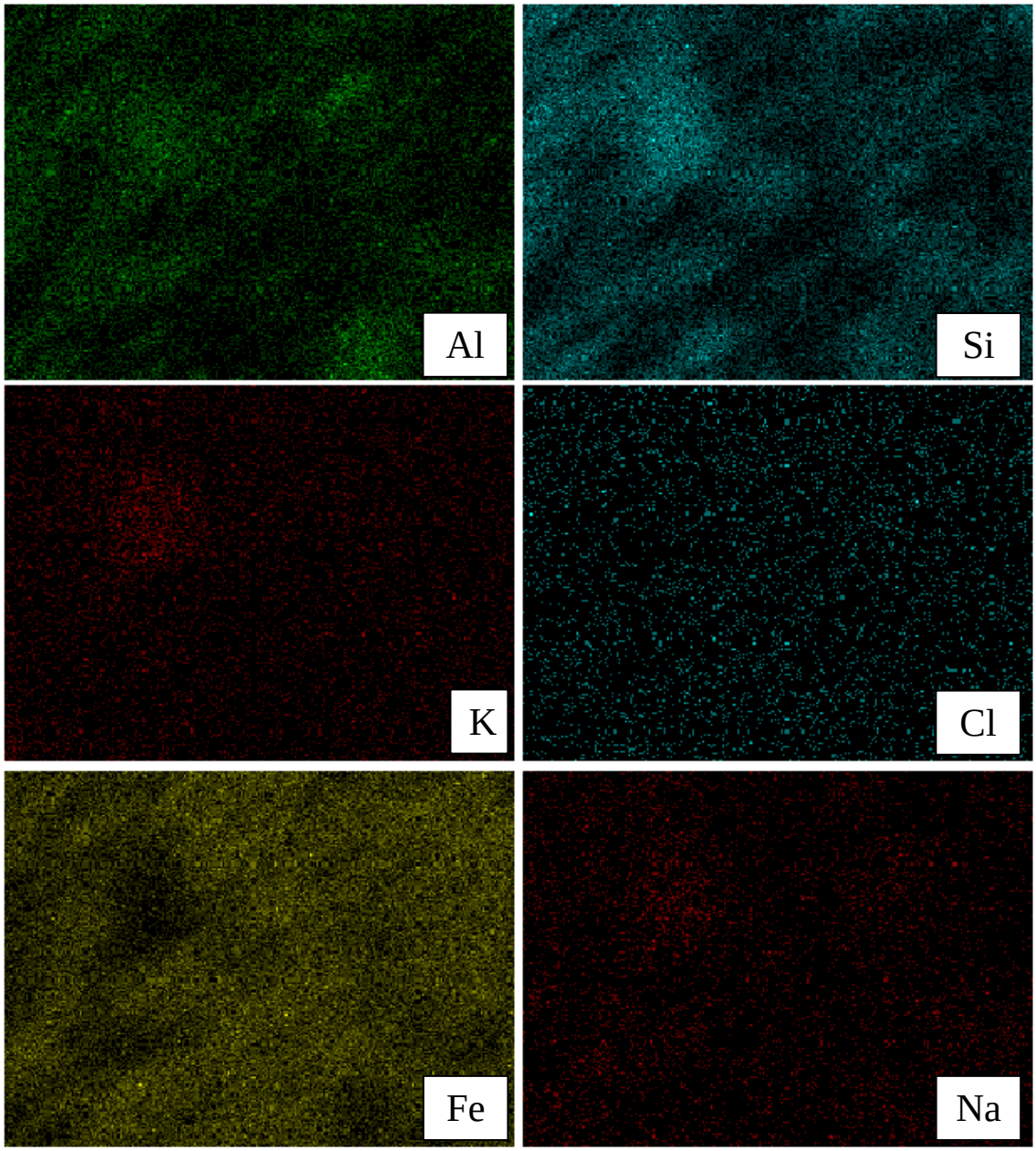

Figure 12 EDX elemental mapping Coal + 40% Biomass T22 180 side.

4.3.3 Sanicro 28 Coal + 40% Biomass 180°

Figure 13 shows elemental maps for Sanicro 28 coal + 40% biomass 180°. The surface mainly consists of Cr and Fe. There are a little deposit which consists of Al and Si. This is different from the T22 samples. On the T22 samples the deposit covered the surface. There are a few larger particles on the surface of Sanicro 28. In Figure 13 a larger particle is show. It consists of Mg, O and S. That could indicate that the particle is magnesium sulfate ($MgSO_4$). There were no presence of K and Cl as shown in Figure 14. That corresponds with the fuel analyses for both the coal and the wood biomass. The analyses showed very small amounts of K and Cl.

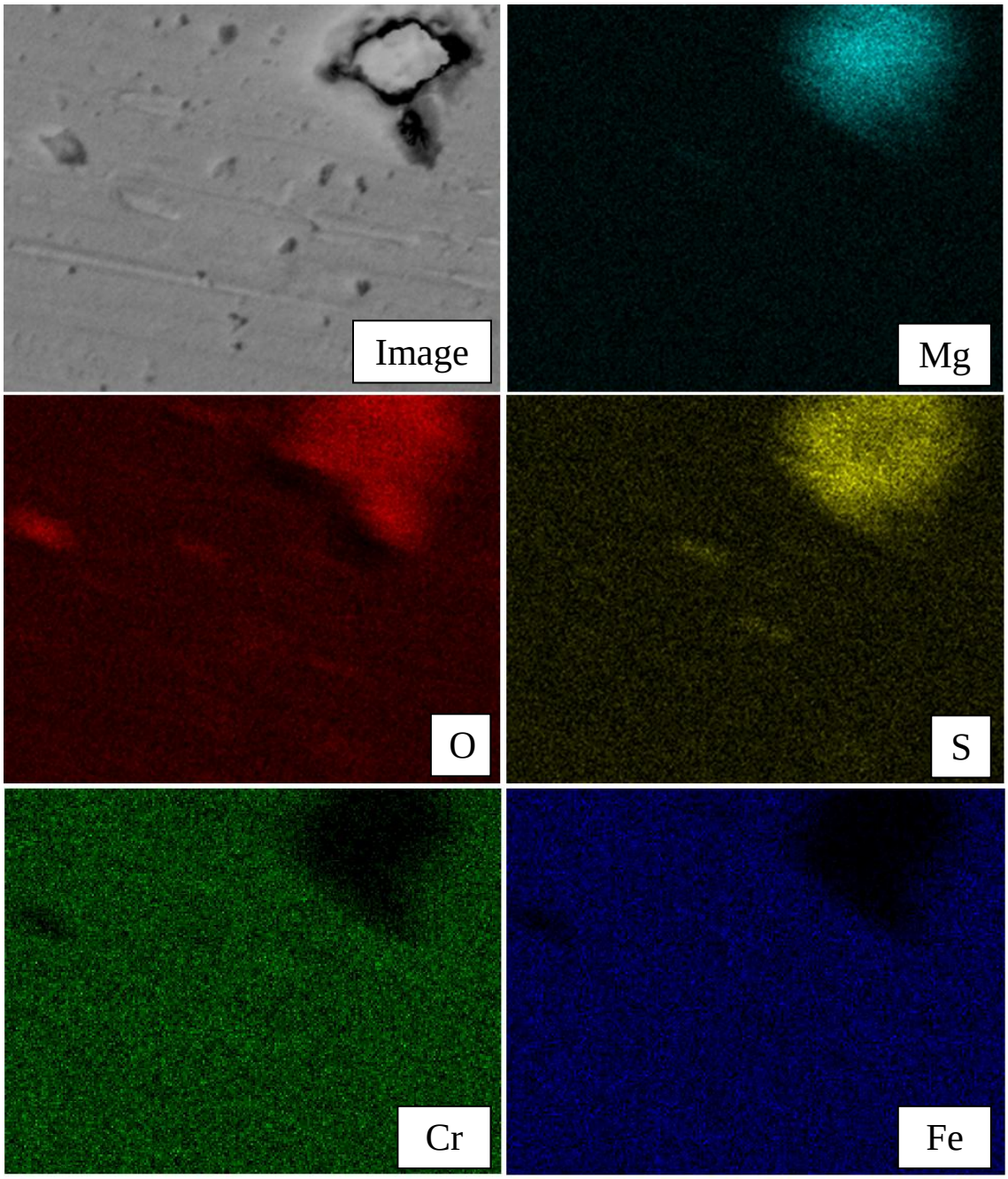

Figure 13 EDX elemental mapping Coal + 40% Biomass Sanicro 28 180 side.

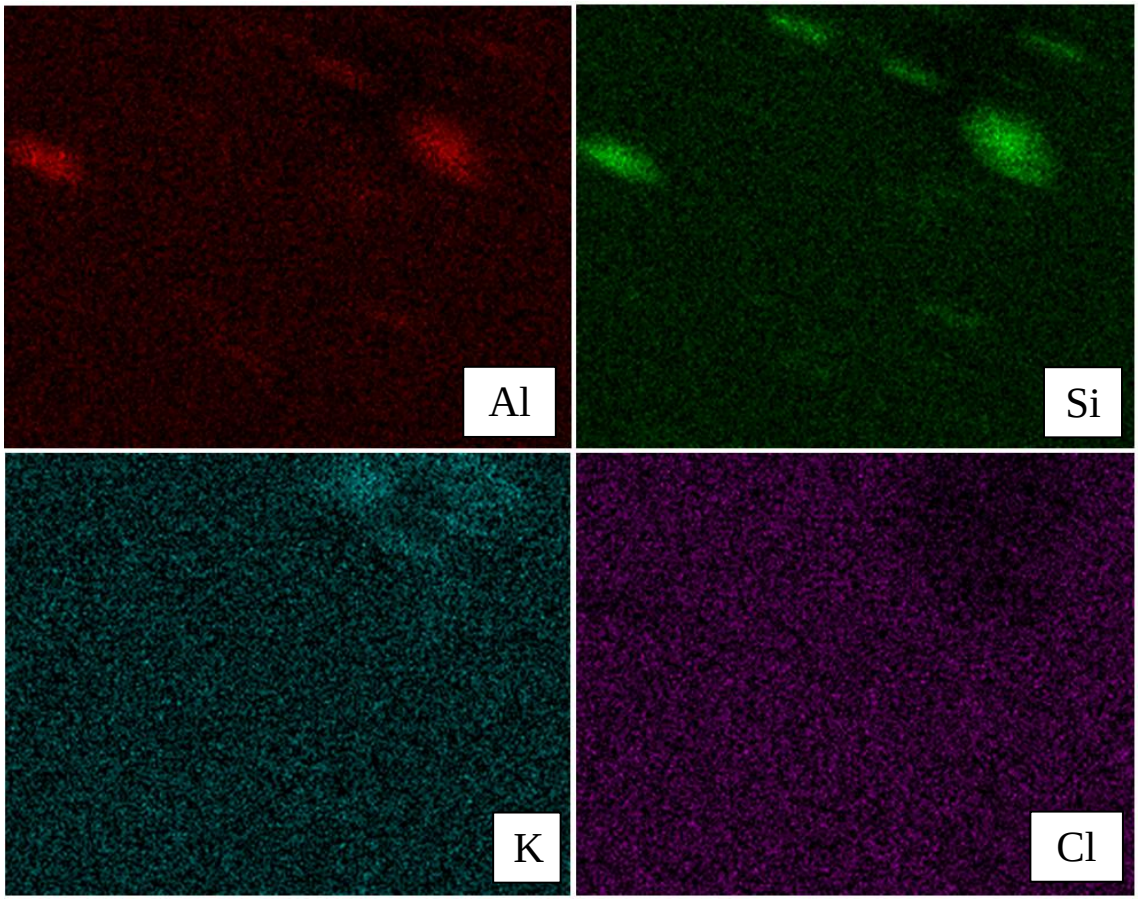

Figure 14 EDX elemental mapping Coal + 40% Biomass Sanicro 28 180 side.

4.3.4 304L Coal + 40% Biomass 180°

Figure 15 show that the surface is Cr and Fe. There is very little Ca on the surface. Also that Al and possibly O is found at the same site. A few oxygen spots and some Al and Si can be found. This is similar to Sanicro 28 with just a few particles on the surface. The other similarity is that there were no K or Cl found on the surface. From the EDX and the SEM images shown before it can be determined that the results for 304L and Sanicro 28 are very similar.

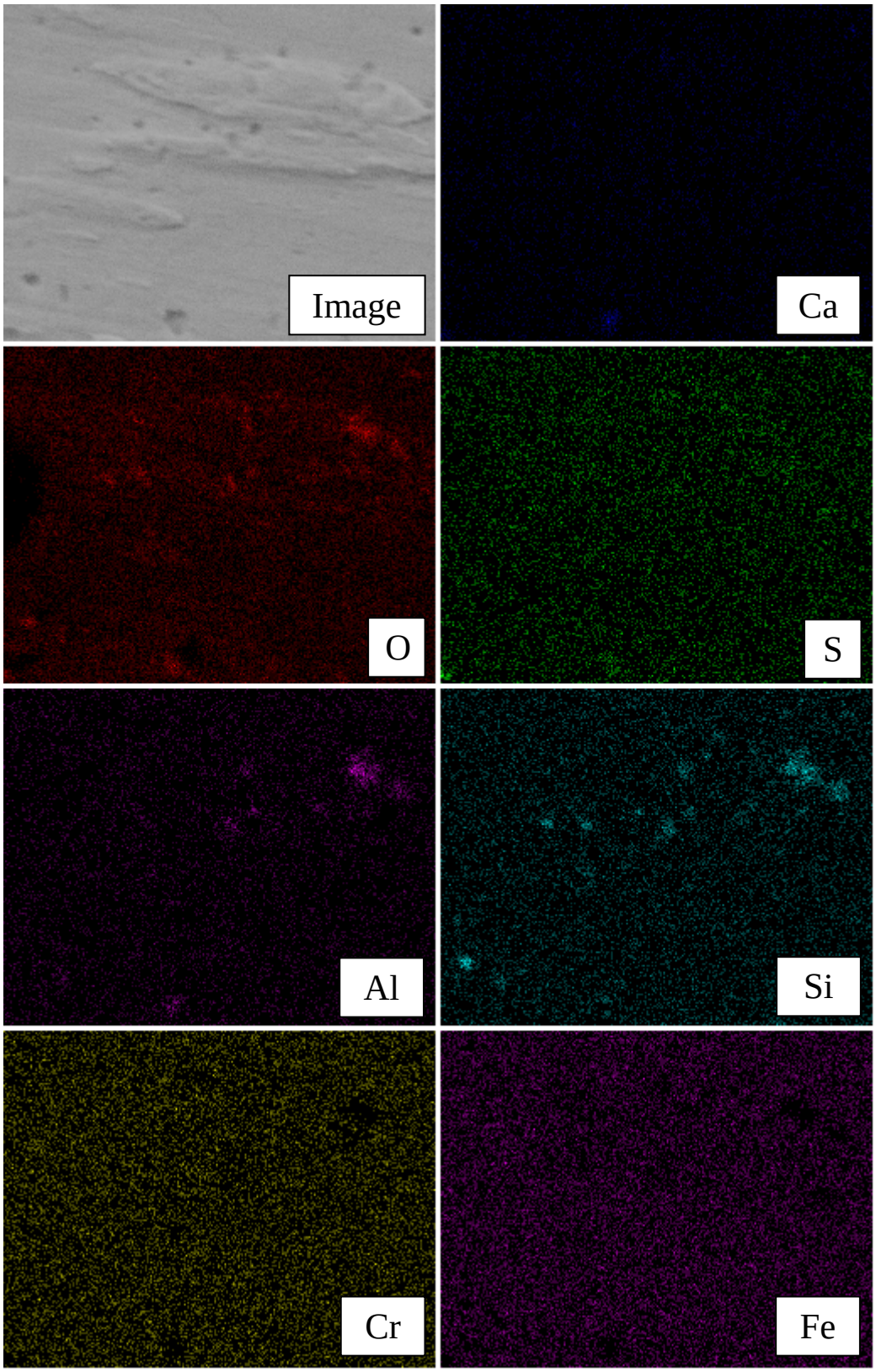

Figure 15 EDX elemental mapping Coal + 40% Biomass 304L 180 side.

4.3.5 Cross Sections SEM & EDX

In order to better evaluate the corrosion attack and possible material loss by observing the cross section area of the ring the sample rings were cut using an automated saw. The T22 samples for all three cases were cut and no corrosion or material loss could be seen from the resulting cross sections. The same was true with the cross-sections for the

other materials in the 40% biomass case. This indicates that it would be possible to substitute some of the coal with wood biomass up to 40% and that no reason can be seen to change the material. This corresponds to previous results in which no signs of corrosion can be seen and also where no corrosive compounds can be found.

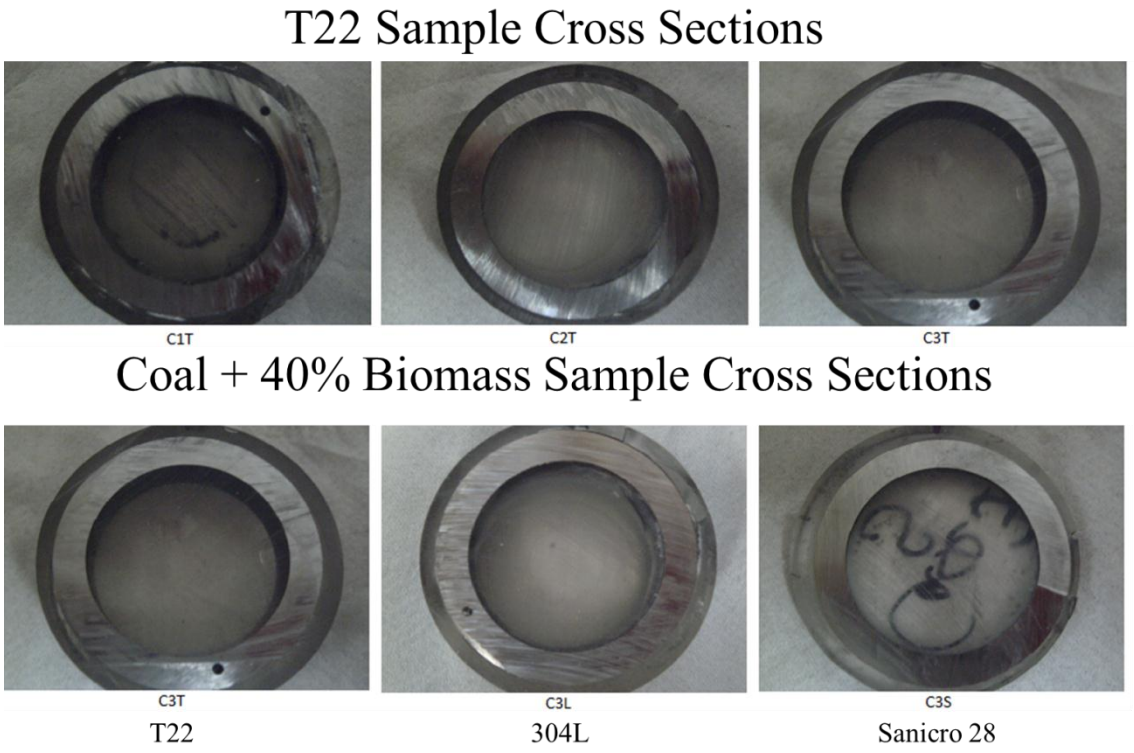

Figure 16 shows an EDX picture of coal + 40% biomass T22 cross-section. It can be seen that some O exist in the boundary between epoxy (on the right) and the ring (on the left). Clear boundaries can be seen for Fe and C showing the clear boundary of metal ring and the epoxy. No S, K or Cl was found with the mapping.

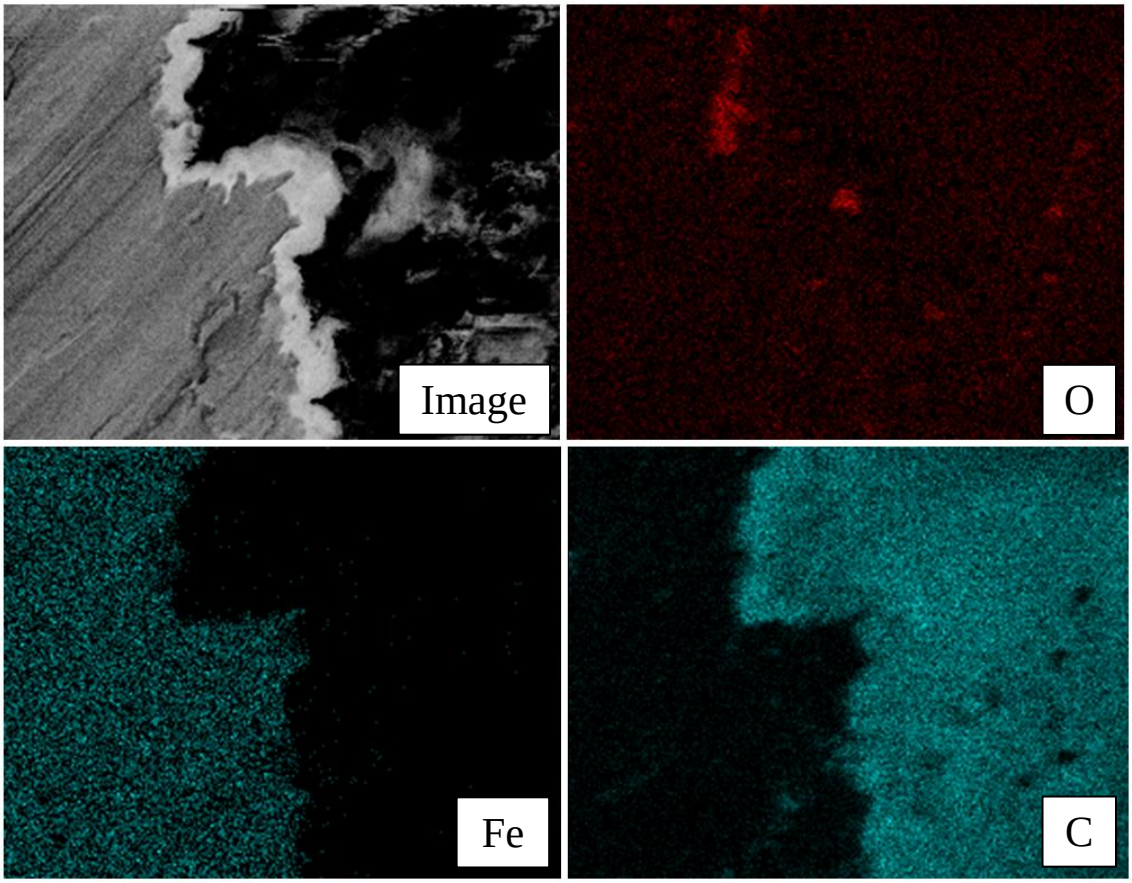

Figure 16 EDX elemental mapping Coal + 40% Biomass T22 cross section.

4.3.6 Gravimetric results

In Table 6 the gravimetric results for the samples before and after exposure are displayed. There is no distinct pattern to the weight change. All changes are less than 0.15 g. As there is no distinct pattern no difference can be detected for either fuel mixture or material. This further confirms the SEM and EDX results. There were no clear difference between the materials and it was possible to use 40% wood biomass in the co-combustion.

Table 6 Gravimetric results of the samples.

Sample	T22 Difference	304L Difference	Sanicro 28 Difference
Case	Wt (g)		
100% Coal	-0.12	0.07	0.01
100% Coal	-0.05	0	-0.02
Coal + 20% Biomass	-0.07	0.01	0.03
Coal + 20% Biomass	-0.05	0.05	0.02
Coal + 40% Biomass	0.02	-0.03	0.02
Coal + 40% Biomass	0.02	-0.02	0.04

The results show that no difference can be detected between the T22 samples from 100% coal and coal + 40% biomass. The same was true for 304L and Sanicro 28, very similar results. There were however differences in regards to deposit between the Cr

rich materials to the T22 samples. There was deposit covering both of the T22 samples surfaces yet very little was found on 304L and Sanicro 28. The gravimetric results confirm that there was very little difference between materials and fuel mixture. It indicates that it would be possible to as much as 40% wood biomass in co-combustion. It also indicates that there would not be an apparent requirement to change the material in the superheaters. However the exposures conducted were only for 24h which only provides the possibility and limited prediction of 40% wood biomass use.

5 Conclusions

- The initial oxidation with 100% coal is similar to coal + 40% biomass which shows that it’s possible to use as much as 40% wood biomass.
- After 24h the overall initial corrosion has been limited.
- No material loss could be detected on the cross-sections.
- The initial corrosion on the wind ward side was more severe than that one the lee ward side.
- Deposit was only detected on the lee ward side.

6 Future work

- Higher temperature with the same biomass.
- Change of biomass with the same temperature and higher temperature.
- Do a serie of experiments with longer run times.
- Cocombustion with only coal and waste.
- Cocombustion with biomass, coal and waste.
- Cocombustion with only biomass and waste.
- Establishing a timeline, reaction paths.
- Possible additives.

References

[1] *BP Statistical Review of World Energy June 2011*

[2] T. Nussbaumer, "*Combustion and Co-combustion of Biomass: Fundamentals, Technologies, and Primary Measures for Emission Reduction*", Energy Fuels, 2003, 17.

[3] S.Q. Turn, C.M. Kinoshita, D.M. lshimura, J Zhou "*The fate of inorganic constituents of biomass in fluidized bed gasification*" Fuel 77, 1998.

[4] J. Pettersson, H. Asteman, J.-E. Svensson, L.-G. Johansson "*KCl Induced Corrosion of a 304-type Austenitic Stainless Steel at 600◦C; The Role of Potassium*" Oxidation of Metals 64, 2005.

[5] M. Montgomery, T. Vilhelmsen, S. A. Jensen, "*Potential high temperature corrosion problems due to co-firing of biomass and fossil fuels*", Materials and Corrosion, 2008, nr 10.

[6] M.A. Uusitalo, P.M.J. Vuoristo, T.A. Ma¨ntyla, "*High temperature corrosion of coatings and boiler steels in oxidizing chlorine-containing atmosphere*", Materials Science and Engineering, 2003, Volume 346.

[7] J.Pettersson , "*Alkali Induced High Temperature Corrosion of Stainless Steel: Experiences from Laboratory and Field*", 2008.

[8] B.M. Jenkins, L.L. Baxter, T.R. Miles Jr, T.R. Miles "*Combustion properties of biomass*", Fuel Processing Technology 54, 1998.

[9] H.P. Michelsen, F. Frandsen, K. Dam-Johansen, O. H. Larsen "*Deposition and high temperature corrosion in a 10 MW straw fired boiler*", Fuel Processing Technology 54, 1998.

[10] M. Hiltunen, V. Barišić, E. Coda Zabetta, "*Combustion of different types of biomass in CFB boilers*", 16th European Biomass Conference, Valencia, Spain, June 2-6, 2008. Available at http://www.fwc.com/publications/tech_papers/files/TP_CFB_08_05.pdf

[11] Oak Ridge National Laboratory, W. B. A. (Sandy) Sharp, SharpConsultant "*SUPERHEATER CORROSION IN BIOMASS BOILERS:Today's Science and Technology*", available at http://www.osti.gov/bridge

[12] P. Henderson, P. Szaka´ los, R. Pettersson, C. Andersson, J. Högberg "*Reducing superheater corrosion in wood-fired boilers*", Materials and Corrosion 57, 2006.

[13] L. Baxter "*Biomass-coal Co-combustion: Opportunity for Affordable Renewable Energy*", Fuel 84, 2005.

[14] D.C. Dayton, B.M. Jenkins, S.Q. Turn, R.R. Bakker, R.B. Williams, D. Belle-Oudry, L.M. Hill "*Release of Inorganic Constituents from Leached Biomass during Thermal Conversion*", Energy & Fuels 13,1999.

[15] A.S. Khanna, "*Introduction to High Temperature Oxidation and Corrosion",* ASM International, 2002.

[16] H.P. Nielsen, F.J. Frandsen, K. Dam-Johansen, L.L. Baxter *"The implications of chlorine-associated corrosion on the operation of biomass-fired boilers"* Progress in Energy and Combustion Science 26, 2000.

[17] H.J. Grabke, E. Reese, M. Spiegel "*The effects of chlorides, hydrogen chloride, and sulfur dioxide in the oxidation of steels below deposits*" Corrosion Science 37, 1995.

[18] H.P. Nielsen, F.J. Frandsen, K. Dam-Johansen, *"Lab-Scale Investigations of High-Temperature Corrosion Phenomena in Straw-Fired Boilers*", Energy & Fuels 13, 1999.

[19] C. Pettersson, J. Pettersson, H. Asteman, J.-E. Svensson, L.-G. Johansson, "*KCl-induced high temperature corrosion of the austenitic Fe–Cr–Ni alloys 304L and Sanicro 28 at 600 °C*", Corrosion Science 48, 2006.

[20] A. Demirbas,” *Combustion characteristics of different biomass fuels*” Progress in Energy and Combustion Science 30, 2004.
[21] D. Zhang, Y. Wang, J-H Liu, H. Yang ”*Performance Test of a 75t/h Circulating Fluidized Bed Boiler Co-Firing Waste*”